An Efficient Numerical Method for Optical Waveguides with Holes

Lijun Yuan and Ya Yan Lu

***Abstract*—Optical waveguides with structural variations along the waveguide axes are useful in many applications. One way to realize such a variation is to insert a sequence of holes in the waveguide core. In this paper, an efficient numerical method is developed for two-dimensional slab waveguides with hole arrays in the core. The method divides the waveguide into a number of segments, then jumps over the holes using the Dirichlet-to-Neumann maps of the segments.**

***Index Terms*—Optical waveguides, Numerical methods, Dirichlet-to-Neumann map.**

I. Introduction

To develop compact waveguide devices for applications in integrated photonic circuits, different approaches that bring large structural changes along the waveguide axis have been explored. A common approach is to change the waveguide geometry discontinuously, so that the refractive index is piecewise constant with respect to the variable z along the waveguide axis [1]–[3]. Another approach is to insert a sequence of holes in the waveguide core [4]–[9]. Some of these structural changes, such as waveguide Bragg gratings, are periodic along the waveguide axis. When defects are inserted in the otherwise periodic structure on the waveguide, resonant transmissions are possible. Such waveguides with embedded microcavities can be used as filters for wavelength division multiplexing applications [8], [9].

Numerical methods are essential to the design and analysis of these waveguiding structures. For a piecewise uniform waveguide where the refractive index is independent of z in each uniform segment, a number of numerical methods are available, including the eigenmode expansion method [10]–[16], the bidirectional beam propagation method [17]–[21] and the Dirichlet-to-Neumann (DtN) map method [22], [23]. These methods are specially designed for piecewise uniform waveguides, and they are more efficient than general purpose methods such as the finite-difference time-domain (FDTD) method. For a waveguide with holes in the core, one approach is to approximate it numerically by a structure with many small uniform (z-invariant) segments. Clearly, this is not an efficient process, since the crude "staircase" approximation to curved dielectric interfaces gives rise to large errors unless the length of the segments (in the z direction) is sufficiently small. This problem is particularly serious for structures with high index contrast and for waves in the transverse magnetic (TM) polarization [24]. Many authors used FDTD to analyze waveguides with holes in the core. However, FDTD requires even more computer resources and its accuracy can be very limited if the interfaces between dielectric and air-holes are not well resolved.

In this paper, we develop an efficient numerical method for two-dimensional (2D) slab waveguides with a finite number of holes in the core. The method is a combination of our earlier technique for photonic crystals [25] and a new technique for truncating the transverse variable. The waveguide is also divided into segments by lines of constant z, but these segments now contain the holes and they are no-longer invariant in z. Like the DtN map method for piecewise uniform waveguides [22], we march two operators (approximated by matrices) from one end of the waveguide to another, based on the DtN maps of the segments. For a segment given by $z_{j-1} < z < z_j$, the DtN map is the operator M (also approximated by a matrix) that maps the wave field to its z derivative at z_{j-1} and z_j. For a uniform segment, a highly accurate Chebyshev collocation method was used to calculate the DtN map M [22]. In Section III, we present an efficient method to calculate M for segments containing holes. This is based on the DtN map for unit cells of photonic crystals [25] and a new three-edge DtN map for boundary cells that can simulate the outgoing radiation condition. In Section IV, we illustrate our method by a number of numerical examples.

II. Operator marching scheme

For 2D problems in the xz plane where the structure is invariant in y, the governing Helmholtz equation is

$$\rho\frac{\partial}{\partial z}\left(\frac{1}{\rho}\frac{\partial u}{\partial z}\right)+\rho\frac{\partial}{\partial x}\left(\frac{1}{\rho}\frac{\partial u}{\partial x}\right)+k_0^2n^2u=0, \qquad (1)$$

where k_0 is the wavenumber in vacuum and $n=n(x,z)$ is the refractive index function. For the transverse electric (TE) polarization, u is the y-component of the electric field and $\rho=1$. For the TM polarization, u is the y-component of the magnetic field and $\rho=n^2$. We consider a slab waveguide with holes in the core. A simple example involving a periodic array of holes in a symmetric slab waveguide is shown in Fig. 1, although our method is applicable to the more general situation where the holes can be different and the array is not periodic. We assume that the z-varying part of the waveguide can be divided into m segments. More precisely, we have $z_0 < z_1 < z_2 < ... < z_m$, such that the j-th segment is given by $z_{j-1} < z < z_j$. Each of these segments may contain one hole in the waveguide core. For $z < z_0$ and $z > z_m$, the structure is z-invariant (straight waveguide) and the refractive index is

L. Yuan and Y. Y. Lu are with the Department of Mathematics, City University of Hong Kong, Kowloon, Hong Kong. This research was partially supported by a grant from City University of Hong Kong (Project No. 7002131).

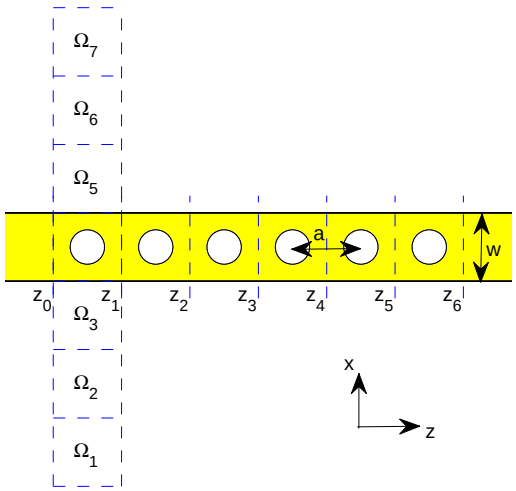

Fig. 1. A symmetric slab waveguide with a periodic array of holes in the core. The vertical dashed lines are used to divide the waveguide into segments. The first segment ($z_0 < z < z_1$) is truncated with 3 cells in each side of the waveguide core.

$n = n_0(x)$ and $n = n_\infty(x)$, respectively. For an incident wave $u^{(i)}$ given in $z < z_0$, our problem is to calculate the transmitted wave for $z > z_m$ and reflected wave for $z < z_0$. To set up proper boundary conditions, we introduce two square root operators,

$$L_l = \left[\rho_l \frac{\partial}{\partial x}\left(\frac{1}{\rho_l}\frac{\partial}{\partial x}\right) + k_0^2 n_l^2(x)\right]^{1/2}, \quad l = 0, \infty,$$

where ρ_0 and ρ_∞ follow the definition of ρ above with the same subscript of n. Then the boundary conditions are [22], [23]:

$$\frac{\partial u}{\partial z} + iL_0\, u = 2iL_0\, u^{(i)}, \quad z = z_0^-, \tag{2}$$

$$\frac{\partial u}{\partial z} - iL_\infty\, u = 0, \qquad z = z_m^+. \tag{3}$$

To allow possible material discontinuities at z_0 and z_m (which is only relevant to the TM case), the boundary conditions are given at z_0^- and z_m^+, respectively.

The DtN map method (or DtN operator marching method) involves two operators Q_j and Y_j at z_j satisfying

$$Q_j\, u_j = \frac{1}{\rho}\frac{\partial u}{\partial z}\bigg|_{z=z_j^-} = \frac{1}{\rho}\frac{\partial u}{\partial z}\bigg|_{z=z_j^+}, \tag{4}$$

$$Y_j\, u_j = u_m, \tag{5}$$

where u is any solution satisfying (1) and (2), $u_j = u(x, z_j)$ and $u_m = u(x, z_m)$. These two operators act on functions of x and they are approximated by matrices when x is discretized. As presented in [22], [23], [25], the DtN map method involves the following steps:

1) initialize Q_m and Y_m as

$$Q_m = \frac{i}{\rho(\cdot, z_m^+)} L_\infty, \quad Y_m = I, \tag{6}$$

2) for $j = m$, ..., 2, 1,

a) calculate the DtN map M of the j-th segment satisfying

$$M \begin{bmatrix} u_{j-1} \\ u_j \end{bmatrix} = \begin{bmatrix} \partial_z u(\cdot, z_{j-1}^+) \\ \partial_z u(\cdot, z_j^-) \end{bmatrix}, \tag{7}$$

b) find Q_{j-1} and Y_{j-1} by

$$Z = [\rho(\cdot, z_j^-) Q_j - M_{22}]^{-1} M_{21}, \tag{8}$$

$$Q_{j-1} = \frac{1}{\rho(\cdot, z_{j-1}^+)}(M_{11} + M_{12} Z), \tag{9}$$

$$Y_{j-1} = Y_j Z, \tag{10}$$

where M_{11}, M_{12}, M_{21} and M_{22} are blocks of M;

3) solve u_0 from

$$[\rho(\cdot, z_0^-)\, Q_0 + iL_0] u_0 = 2iL_0\, u^{(i)}(\cdot, z_0^-); \tag{11}$$

4) find the reflected and transmitted waves by

$$u^{(r)}(\cdot, z_0^-) = u_0 - u^{(i)}(\cdot, z_0^-), \tag{12}$$

$$u^{(t)}(\cdot, z_m) = u_m = Y_0\, u_0. \tag{13}$$

Notice that Q_m in (6) comes from the boundary condition (3), the marching formulas (9) and (10) are derived by replacing the z derivatives in (7), and Eq. (11) is the boundary condition (2).

III. DtN map of the segments

In this section, we describe an efficient method for computing the DtN map M for each segment. First, we truncate the transverse variable x, then partition the segment into a finite number of rectangular or square cells. A typical example with seven cells is shown in Fig. 1 for the first segment. The cell at the center of the segment corresponds to the waveguide core with a single hole, and the other cells cover the cladding or substrate. Let us consider the first segment given by $z_0 < z < z_1$ and assume that it has a partition of p cells separated by the lines $x = x_k$ for $0 \le k \le p$. More precisely, the k-th cell is the rectangle (or square) given by

$$\Omega_k = \{(x, z) \mid x_{k-1} < x < x_k,\ z_0 < z < z_1\}.$$

We first calculate DtN maps of the cells, then merge their DtN maps to find the DtN map M of the segment.

The DtN map of a closed domain Ω is the operator Λ such that $\Lambda u = \partial_\nu u$ on $\partial\Omega$ for any u satisfying the Helmholtz equation (1), where $\partial\Omega$ is the boundary of Ω and ν is a unit normal vector of $\partial\Omega$. For the rectangular cell Ω_k, we take the normal derivative to be the x- or z-derivative and avoid the four corners. To allow possible dielectric interfaces on the boundary of Ω_k, the normal derivative is obtained in a limit from the inside of Ω_k. More precisely, the DtN map $\Lambda^{(k)}$ of the cell Ω_k for $1 < k < p$, satisfies

$$\Lambda^{(k)} \begin{bmatrix} u_{0k} \\ v_{k-1} \\ u_{1k} \\ v_k \end{bmatrix} = \begin{bmatrix} \partial_z u_{0k}^+ \\ \partial_x v_{k-1}^+ \\ \partial_z u_{1k}^- \\ \partial_x v_k^- \end{bmatrix}, \tag{14}$$

where

$$u_{0k} = u(x, z_0), \quad \partial_z u_{0k}^+ = \partial_z u(x, z_0^+),$$
$$u_{1k} = u(x, z_1), \quad \partial_z u_{1k}^- = \partial_z u(x, z_1^-),$$

for $x_{k-1} < x < x_k$, and

$$v_{k-1} = u(x_{k-1}, z), \quad \partial_x v_k^- = \partial_x u(x_k^-, z),$$
$$v_k = u(x_k, z), \qquad \partial_x v_{k-1}^+ = \partial_x u(x_{k-1}^+, z)$$

for $z_0 < z < z_1$. In practice, $\Lambda^{(k)}$ is approximated by a matrix in connection with a discretization of x and z. If we use N_z sampling points for $z \in (z_0, z_1)$ and $N_x^{(k)}$ points for $x \in (x_{k-1}, x_k)$, the total number of sampling points on the boundary of Ω_k is $J = 2(N_z + N_x^{(k)})$, the operator $\Lambda^{(k)}$ is then approximated by a $J \times J$ matrix. As described in [25], the matrix $\Lambda^{(k)}$ is obtained by assuming that the general solution of Helmholtz equation (1) in Ω_k can be approximated by a sum of J special solutions. That is,

$$u(\mathbf{x}) \approx \sum_{l=1}^{J} c_l \phi_l(\mathbf{x}), \quad \mathbf{x} = (x, z) \in \Omega_k,$$

where ϕ_1, ϕ_2, ..., are the special solutions of (1). If we order the J sampling points on the boundary of Ω_k as $\mathbf{x}_s$ for $s =$ 1, 2, ..., J, and evaluate ϕ_l and the normal derivative of ϕ_l at these points, we obtain two matrices Λ_1 and Λ_2 whose (s, l) entries are $\phi_l(\mathbf{x}_s)$ and $\partial_\nu \phi_l(\mathbf{x}_s)$ respectively, where ∂_ν is either ∂_x or ∂_z. The DtN map of Ω_k is then obtained as $\Lambda^{(k)} = \Lambda_2 \Lambda_1^{-1}$. For cells containing a circular hole and empty cells of a homogeneous medium, we use cylindrical waves as the special solutions. If the hole has a more general shape, a boundary integral equation method can be used to find the special solutions [26].

The first cell Ω_1 and the last cell Ω_p require special treatment. Since x is truncated to $x_0 < x < x_p$, we should impose outgoing radiation conditions at x_0 and x_p. If the medium is homogeneous in the half plane $x < x_1$, the wave field there is a linear combination of plane waves propagating towards $x = -\infty$ and evanescent plane waves that decay exponentially as $x \to -\infty$. That is

$$u(x, z) = \int_{-\infty}^{\infty} A(\beta) e^{i(-\alpha x + \beta z)} d\beta \quad \text{for} \quad x < x_1, \qquad (15)$$

where $\alpha = \sqrt{k_0^2 n^2 - \beta^2}$ (which becomes $\alpha = i\sqrt{\beta^2 - k_0^2 n^2}$ if $|\beta| > k_0 n$), n is the constant refractive index for $x < x_1$ and A is the unknown amplitude depending on β. Therefore, we can choose some discrete values for β and approximate the wave field in Ω_1 by a finite sum of (both propagating and evanescent) plane waves:

$$u(x, z) \approx \sum_{l=1}^{J} c_l e^{i(-\alpha_l x + \beta_l z)} \quad \text{for} \quad (x, z) \in \Omega_1. \qquad (16)$$

In the above, β_l is real, $\alpha_l = \sqrt{k_0^2 n^2 - \beta_l^2}$ can be real or imaginary and J is the number of plane waves. Typically, we choose β_l uniformly in the interval $(-\gamma k_0 n, \gamma k_0 n)$ where γ is a parameter, e.g. $\gamma = 2$. Since we attempt to approximate the outgoing radiation condition at $x = x_0$, we construct a DtN map for Ω_1 involving only three edges, that is, without the edge at $x = x_0$. We have

$$\Lambda^{(1)} \begin{bmatrix} u_{01} \\ u_{11} \\ v_1 \end{bmatrix} = \begin{bmatrix} \partial_z u_{01}^+ \\ \partial_z u_{11}^- \\ \partial_x v_1^- \end{bmatrix}. \qquad (17)$$

Using N_z sampling points for $z \in (z_0, z_1)$, $N_x^{(1)}$ sampling points for $x \in (x_0, x_1)$ and $J = N_z + 2N_x^{(1)}$ plane waves in (16), we approximate $\Lambda^{(1)}$ by a $J \times J$ matrix. Similarly, the DtN map for Ω_p is constructed from plane waves that propagate towards $x = +\infty$ or evanescent waves that decay as x is increased, and it involves only three edges (without the edge at $x = x_p$). We have

$$\Lambda^{(p)} \begin{bmatrix} u_{0p} \\ v_{p-1} \\ u_{1p} \end{bmatrix} = \begin{bmatrix} \partial_z u_{0p}^+ \\ \partial_x v_{p-1}^+ \\ \partial_z u_{1p}^- \end{bmatrix}. \qquad (18)$$

If J is relatively large, it may be difficult to construct the DtN map $\Lambda^{(1)}$ from the plane waves in (16) directly, since the vectors obtained by evaluating the plane waves at the sampling points on the boundary may lose linear independence. In that case, we divide Ω_1 into four sub-cells, then use the plane waves to construct the DtN maps of the two sub-cells near the boundary at x_0 and cylindrical waves for the other two sub-cells. The DtN maps of the four sub-cells are then combined to obtain the DtN map of Ω_1. We can also include the perfectly matched layer (PML) technique [27] in the construction of boundary DtN maps. To set up boundary conditions at z_0^- and z_m^+, we need PMLs to terminate the x axis. To avoid inconsistency at z_0 and z_m, we use PMLs for the entire structure. This can be easily done based on the complex coordinate stretching formulation [28] of PML. In that case, the transverse variable x is replaced by a complex $\hat{x}$ and we simply replace x by $\hat{x}$ in Eq. (16).

With the DtN maps of the cells, we can calculate the DtN map of the segment by a merging process described in [29]. Let us introduce three vectors

$$v = \begin{bmatrix} v_1 \\ v_2 \\ \vdots \\ v_{p-1} \end{bmatrix}, \quad u_0 = \begin{bmatrix} u_{01} \\ u_{02} \\ \vdots \\ u_{0p} \end{bmatrix}, \quad u_1 = \begin{bmatrix} u_{11} \\ u_{12} \\ \vdots \\ u_{1p} \end{bmatrix}. \qquad (19)$$

The merging process is given in the following steps:

1) set up a linear system for v, u_0 and u_1;
2) solve v in terms of u_0 and u_1;
3) express $\partial_z u_0$ and $\partial_z u_1$ by u_0, u_1 and v,
4) eliminate v to obtain M.

In Step 1, an equation for $v_k = u(x_k, z)$ $(1 \le k < p)$ can be established from the continuity of $\rho^{-1}\partial_x u$ at $x = x_k$ and evaluating $\partial_x v_k^\pm$ using the DtN maps of Ω_k and Ω_{k-1}. Step 3 is simply a re-arrangement of $\partial_z u_{0k}^+$ and $\partial_z u_{1k}^-$ given in the definition of the DtN maps $\Lambda^{(k)}$ for $1 \le k \le p$. More details of the merging process can be found in [29].

IV. Numerical examples

In this section, we illustrate our method by a few examples. The first example involves a periodic array of holes as shown

in Fig. 1. We have a symmetric slab waveguide with air claddings. The width and the refractive index of the waveguide core are $w = 0.47\,\mu$m and $n = \sqrt{10.1}$, respectively. In the waveguide core, we have a periodic array of 8 air-holes with the radius $r = 0.15\,\mu$m, and the period is $a = 0.42\,\mu$m. The centers of these holes are located on the central line of the waveguide core.

In our numerical implementation, the structure is divided into $m = 8$ segments by the vertical lines $z = z_j$ for $0 \le j \le m$, where $z_j - z_{j-1} = a$. Each segment contains exactly one air-hole in the waveguide core. The vertical lines are chosen so that the center of the air-hole in the segment given by $z_{j-1} < z < z_j$ is located at the midpoint $(z_{j-1} + z_j)/2$. The waveguide core (with an air-hole inside) is a rectangular cell of the segment. We truncate the x variable so that the segment contains $p = 11$ cells (five cells on each side of the waveguide core) and assume that all cells have the same size: length a in the z direction and width w in the x direction. For this example, we can use a small number of cells on each side of the waveguide core, since the propagating mode of the slab waveguide (without holes) decays rapidly in the transverse direction and our special boundary cell can approximate outgoing radiation waves accurately. For discretization, we use $N_z = N_x = 10$ points to sample the horizontal and vertical edges of each cell. The total number of sampling points in the x direction is thus $p \times N_x = 110$. Therefore, the operators Q_j and Y_j are approximated by 110×110 matrices. To initialize Q_m in the DtN operator marching scheme and to solve u at z_0 once Q_0 is obtained, we need the square root operator ($L_0 = L_\infty$ here). For that purpose, we use a fourth order finite difference method [30] to approximate the transverse differential operator by a matrix based on the same set of sampling points of x, then calculate the square root of the matrix using its eigenvalue decomposition. To reduce reflections due to the truncation of the x variable, we use a perfectly matched layer (PML) [27] of $0.47\,\mu$m at each end of the x interval. The parameters used in the PML are chosen following the procedure in [31]. In Fig. 2, we show the transmission and reflection spectra for the TE polarization, where the incident wave is the fundamental mode of the z-invariant waveguide without the holes. The results in Fig. 2 are confirmed by additional calculations using more cells in each segment and more sampling points on each edge of the cells.

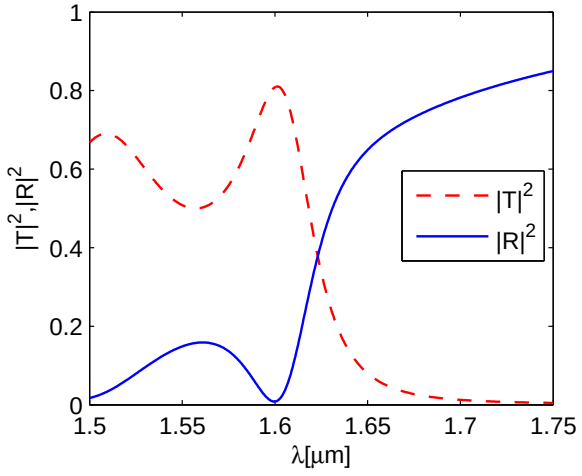

Fig. 2. The transmission and reflection spectra of a symmetric slab waveguide with 8 holes in the core. T and R are the normalized amplitudes of the fundamental mode in the transmitted and reflected waves.

Next, we consider some examples originally analyzed in [8]. Three structures are shown in Fig. 3 and they are formed by embedding a series of air-holes in a symmetric slab waveguide with air claddings. The refractive index and the width of waveguide core are $n = 3.3$ and $w = 0.26\,\mu$m, respectively, and the radius of the air-holes is $r = 0.067\,\mu$m. The air-holes are arranged along the central line of the waveguide core. The normal distance between two nearby air-holes is $a = 0.215\,\mu$m. However, the distance may be increased to $d = 0.26\,\mu$m to create a microcavity in the waveguide. Structure (a) has 6 air-holes and one microcavity at the center. Both structures (b) and (c) have two microcavities, and they have 8 and 11 air-holes, respectively.

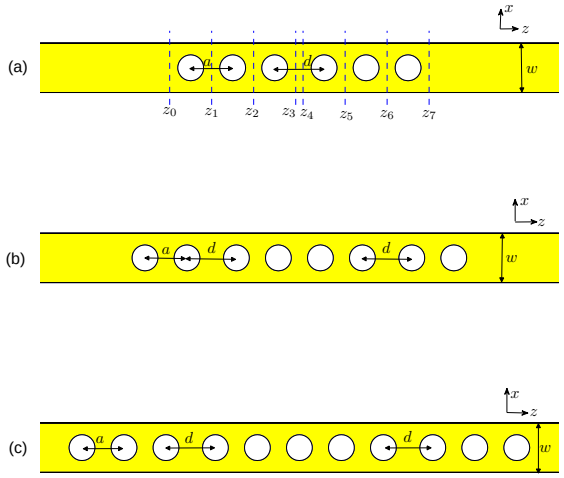

Fig. 3. Waveguide structures with air-holes in the core originally analyzed in [8]. Microcavities are created by increasing the distance between neighboring air-holes from a to d.

To use the DtN map method developed in Sections II and III, we divide each structure into m segments, where m is the number of holes plus the number of microcavities. There are only two different types of segments, namely, the segments containing air-holes in the middle and the z-invariant segments of the microcavities. The lengths (in the z-direction) of these two types of segments are a and $d - a$, respectively. The transverse variable x is truncated to cover 9 cells of the same size in each segment or 4 cells in each side of the waveguide core. In the fully discrete case, each vertical edge of length w is sampled by $N_x = 8$ points, while a horizontal edge is sampled by $N_z = 8$ points for segments with holes and $N_z = 3$ points for segments of the microcavities. Therefore, the total number of discrete points in the x direction is 72. As before, for boundary conditions at z_0 and z_m, we use a fourth order finite difference scheme [30] and PMLs of width

w to discretize the transverse operator based on the same set of points for x. In Fig. 4, we show the transmission spectra

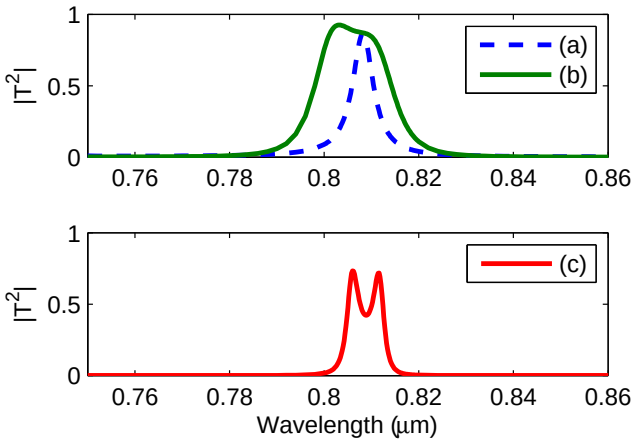

Fig. 4. Transmission spectra for structures (a), (b) and (c) shown in Fig. 3, where T is the amplitude of the fundamental TM mode of the transmitted wave.

of these three structures for the TM polarization, where the incident wave is the fundamental mode of the slab waveguide without holes. For the first two structures, our results agree reasonably well with the FDTD results reported in [8]. For structure (c), the transmission spectra we obtained does not have a flat top. We have validated the results in Fig. 4 by separate calculations based on the eigenmode expansion method using up to 200 z-invariant segments for each hole.

V. Conclusion

In this paper, we developed a DtN map method for 2D slab waveguides with an array of holes in the waveguide core. The 2D structures we studied can be regarded as models for true three dimensional waveguide structures reported in [5], [7]–[9]. The DtN map method was previously used to study finite photonic crystals in [25] and piecewise uniform waveguides in [22], [23]. The segments used in this paper are different, since they are unbounded in the transverse direction and contain holes. To find the DtN map for such a segment, we divide it into a number of cells and merge the DtN maps of these cells. A special construction for boundary cells was developed to simulate the outgoing radiation condition. Although we have to manipulate a pair of operators Q_j and Y_j, they can be approximated by matrices of relatively small sizes. Existing numerical methods for piecewise uniform waveguides are not very efficient if a large number of z-invariant segments with different refractive index profiles are involved. In particular, the eigenmode expansion method would require the solution of eigenmodes for all different profiles. Overall, our method is efficient because it jumps over the holes, instead of approximating each hole by many small z-invariant segments.

References

[1] T. F. Krauss, B. Vogele, C. R. Stanley, R. M. De la Rue, "Waveguide microcavity based on photonic microstructures," *IEEE Photonics Technology Letters*, vol. 9, no. 2, pp. 176-178, Feb. 1997.

[2] J. Ctyroky, S. Helfert, R. Pregla, P. Bienstman, R. Baets, R. De Ridder, R. Stoffer, G. Klaasse, J. Petracek, P. Lalanne, J. P. Hugonin and R. M. De La Rue, "Bragg waveguide grating as a 1D photonic band gap structure: COST 268 modelling task," *Optical and Quantum Electronics*, vol. 34, no. 5, pp. 455-470, 2002.

[3] M. Gnan, G. Bellanca, H. M. H. Chong, P. Bassi and R. M. De la Rue, "Modelling of photonic wire Bragg gratings," *Optical and Quantum Electronics*, vol. 38, pp. 133-148, Jan. 2006.

[4] P. R. Villeneuve, S. H. Fan, J. D. Joannopoulos, K. Y. Lim, G. S. Petrich, L. A. Kolodziejski and R. Reif, "Air-bridge microcavities," *Applied Physics Letters*, vol. 67, no. 2, pp. 167-169, July 1995.

[5] J. P. Zhang, D. Y. Chu, S. L. Wu, W. G. Bi, R. C. Tiberio, R. M. Joseph, A. Taflove, C. W. Tu and S. T. Ho, "Nanofabrication of 1-D photonic bandgap structures along a photonic wire," *IEEE Photonics Technology Letters*, vol. 8, no. 4, pp. 491-493, Apr. 1996.

[6] J. C. Chen, H. A. Haus, S. H. Fan, P. R. Villeneuve, and J. D. Joannopoulos, "Optical filters from photonic band gap air bridges," *Journal of Lightwave Technology*, vol. 14, no. 11, pp. 2575-2580, Nov. 1996.

[7] J. S. Foresi, P. R. Villeneuve, J. Ferrera, E. R. Thoen, G. Steinmeyer, S. Fan, J. D. Joannopoulos, L. C. Kimerling, H. I. Smith and E. P. Ippen, "Photonic-bandgap microcavities in optical waveguides," *Nature*, vol. 390, no. 6656, pp. 143-145, 1997.

[8] A. S. Jugessur, P. Pottier and R. M. De La Rue, "Engineering the filter response of photonic crystal microcavity filters," *Optics Express*, vol. 12, no. 7, pp. 1304-1312, Apr. 2004.

[9] C. H. Chen and Y. Fainman, "Photonic bandgap microcavities with flat-top response," *IEEE Journal of Selected Topics in Quantum Electronics*, vol. 13, no. 2, pp. 262-269, Mar./Apr. 2007.

[10] Q. H. Liu and W. C. Chew, "Analysis of discontinuities in planar dielectric waveguides: an eigenmode propagation method", *IEEE Transactions on Microwave Theory and Techniques*, vol. 39, no. 3, pp. 422-430, March 1991.

[11] G. Sztefka and H. P. Nolting, "Bidirectional eigenmode propagation for large refractive index steps," *IEEE Photonics Technology Letters*, vol. 5, pp. 554-557, 1993.

[12] J. Willems, J. Haes and R. Baets, "The bidirectional mode expansion method for 2-dimensional wave-guides - the TM case," *Optical and Quantum Electronics*, vol. 27, pp. 995-1007, Oct. 1995.

[13] S. F. Helfert and R. Pregla, "Efficient analysis of periodic structures," *Journal of Lightwave Technology*, vol. 16, pp. 1694-1702, Sept. 1998.

[14] P. Bienstman and R. Baets, "Optical modelling of photonic crystals and VCSELs using eigenmode expansion and perfectly matched layers," *Opt. Quant. Electron.*, vol. 33, pp. 327-341, April 2001.

[15] E. Silberstein, P. Lalanne, J. P. Hugonin and Q. Cao, "Use of grating theories in integrated optics," *J. Opt. Soc. Am. A*, vol. 18, pp. 2865-2875, Nov. 2001.

[16] J. Čtyroký, "Improved bidirectional mode expansion propagation algorithm based on Fourier series," *Journal of Lightwave Technology*, vol. 25, no. 9, pp. 2321-2330, Sept. 2007.

[17] H. Rao, R. Scarmozzino and R. M. Osgood, "A bidirectional beam propagation method for multiple dielectric interfaces," *IEEE Photonics Technology Letters*, vol. 11, no. 7, pp. 830-832, 1999.

[18] H. El-Refaei, D. Yevick and I. Betty, "Stable and noniterative bidirectional beam propagation method," *IEEE Photonics Technology Letters*, vol. 12, pp. 389-391, 2000.

[19] P. L. Ho and Y. Y. Lu, "A stable bidirectional propagation method based on scattering operators," *IEEE Photon. Technol. Lett.*, vol. 13, no. 12, pp. 1316-1318, 2001.

[20] P. L. Ho and Y. Y. Lu, "A bidirectional beam propagation method for periodic waveguides," *IEEE Photon. Technol. Lett.*, vol. 14, pp. 325-327, March 2002.

[21] Y. Y. Lu and S. H. Wei, "A new iterative bidirectional beam propagation method", *IEEE Photonics Technology Letters*, vol. 14, no. 11, pp. 1533-1535, Nov. 2002.

[22] L. Yuan and Y. Y. Lu, "An efficient bidirectional propagation method based on Dirichlet-to-Neumann maps," *IEEE Photonics Technology Letters*, vol. 18, pp. 1967-1969, Sept. 2006.

[23] L. Yuan and Y. Y. Lu, "A recursive doubling Dirichlet-to-Neumann map method for periodic waveguides," *Journal of Lightwave Technology*, vol. 25, pp. 3649-3656, Nov. 2007.

[24] E. Popov, M. Nevière, B. Gralak and G. Tayeb, "Staircase approximation validity for arbitrary-shaped gratings", *J. Opt. Soc. Am. A*, vol. 19, no. 1, pp. 33-42, Jan. 2002.

[25] Y. Huang and Y. Y. Lu, "Scattering from periodic arrays of cylinders by Dirichlet-to-Neumann maps," *Journal of Lightwave Technology*, vol. 24, pp. 3448-3453, 2006.

[26] J. Yuan, Y. Y. Lu and X. Antoine, "Modeling photonic crystals by boundary integral equations and Dirichlet-to-Neumann maps," *Journal of Computational Physics*, vol. 227, no. 9, pp. 4617-3629, 2008.

[27] J. P. Berenger, "A perfectly matched layer for the absorption of electromagnetic waves", *Journal of Computational Physics*, vol. 114, no. 2, pp. 185-200, 1994.

[28] W. C. Chew and W. H. Weedon, "A 3D perfectly matched medium from modified Maxwells equations with stretched coordinates", *Microwave and Optical Technology Letters*, vol. 7, no. 13, pp. 599-604, 1994.

[29] Y. Huang, Y. Y. Lu and S. Li, "Analyzing photonic crystal waveguides by Dirichlet-to-Neumann maps," *Journal of the Optical Society of America B*, vol. 24, no. 11, pp. 2860-2867, Nov. 2007.

[30] Y. P. Chiou, Y. C. Chiang and H. C. Chang, "Improved three-points formulas considering the interface conditions in the finite-difference analysis of step-index optical devices," *J. Lightwave Technology*, vol. 18, no. 2, pp. 243-251, 2000

[31] Y. Y. Lu, "Minimizing the discrete reflectivity of perfectly matched layers," *IEEE Photonics Technology Letters*, vol. 18, no. 3, pp. 487-489, 2006.